Available online at www.sciencedirect.com
SCIENCE DIRECT®
Hearing Research 207 (2005) 22–34
HEARING RESEARCH
www.elsevier.com/locate/heares

Differential distribution of β- and γ-actin in guinea-pig cochlear sensory and supporting cells

D.N. Furness [a,*], Y. Katori [b], S. Mahendrasingam [a], C.M. Hackney [a,c]

[a] MacKay Institute of Communication and Neuroscience, School of Life Sciences, Keele University, Staffordshire ST5 5BG, United Kingdom
[b] Department of Otolaryngology and Head & Neck Surgery, Tohoku University, Graduate School of Medicine, 1-1 Seiryo-machi, Aoba, Sendai 980-8574, Japan
[c] Department of Anatomy, University of Wisconsin-Madison, 1300 University Avenue, Madison, WI 53706, USA

Received 10 May 2005; accepted 12 May 2005
Available online 15 July 2005

Abstract

Sensory and supporting cells of the mammalian organ of Corti have cytoskeletons containing β- and γ-actin isoforms which have been described as having differing intracellular distributions in chick cochlear hair cells. Here, we have used post-embedding immunogold labelling for β- and γ-actin to investigate semiquantitatively how they are distributed in the guinea-pig cochlea and to compare different frequency locations. Amounts of β-actin decrease and γ-actin increase in the order, outer pillar cells, inner pillar cells, Deiters' cells and hair cells. There is also more β-actin and less γ-actin in outer pillar cells in higher than lower frequency regions. In hair cells, β-actin is present in the cuticular plate but is more concentrated in the stereocilia, especially in the rootlets and towards the periphery of their shafts; labelling densities for γ-actin differ less between these locations and it is the predominant isoform of the hair-cell lateral wall. Alignments of immunogold particles suggest β-actin and γ-actin form homomeric filaments. These data confirm differential distribution of these actin isoforms in the mammalian cochlea and reveal systematic differences between sensory and supporting cells. Increased expression of β-actin in outer pillar cells towards the cochlear base may contribute to the greater stiffness of this region.

Keywords: Isoactins; Actin filaments; Auditory system; Hair cells; Stereocilia

1. Introduction

Actin is a major component of hair cells and supporting cells in the inner ear. In the mammalian cochlea, various properties of these cells change systematically along the length of the cochlear partition (see e.g. Lim, 1986). These changes contribute to the processes by which complex sounds are decomposed into their component frequencies (Robles and Ruggero, 2001). Morphological changes in actin-containing structures along the cochlear length have been reported (Carlisle et al., 1988) but whether specific variations occur in the types and amount of actin present has yet to be investigated.

Three subtypes of actin, α, β and γ, are distinguishable by their differing isoelectric points on 2D gels (Vandekerckhove and Weber, 1978, 1981). Six functional actin genes have been described in humans, four of which encode the α- and γ-isoforms found in different muscle types (see e.g. Herman, 1993). The remaining two, *ACTB* and *ACTG1*, code for cytoplasmic β- and γ-actin which are found in a wide range of cell types including

Abbreviations: FITC, Fluorescein isothiocyanate; GS-PBS, goat serum in phosphate buffered saline; IHC, inner hair cell; MAP, microtubule associated protein; OHC, outer hair cell; PB, phosphate buffer; PBS, phosphate buffered saline; STBS, serum in TRIS buffered saline; TBS, TRIS buffered saline; TEM, transmission electron microscope; TRITC, tetramethyl rhodamine isothiocyanate

* Corresponding author. Tel.: +44 1782 583496; fax: +44 1782 583055.
E-mail address: coa14@keele.ac.uk (D.N. Furness).

0378-5955/$ - see front matter © 2005 Elsevier B.V. All rights reserved.
doi:10.1016/j.heares.2005.05.006

hair cells and supporting cells (Slepecky and Savage, 1994; Nakazawa et al., 1995; Hofer et al., 1997). Mutations of the human γ-actin gene cause progressive non-syndromic sensorineural hearing loss, DFNA20/26 (Zhu et al., 2003; Wijk et al., 2003). Given the widespread distribution of γ-actin in the body, this is surprising and implies that it has a special role in hearing.

The cytoplasmic isoforms, β- and γ-actin, differ in proportion and distribution in various tissues (e.g. Otey et al., 1987) and interact with specific associated proteins (Sheterline et al., 1998). Changes in their expression result in cell phenotype changes, emphasizing their role in maintaining morphology (see review by Khaitlina, 2001). In the brain, β-actin is restricted to dynamic structures and is associated with cell processes e.g., dendritic spines and growth cone filopodia, whereas γ-actin is more ubiquitously distributed and occurs in relatively quiescent regions (Micheva et al., 1998).

In auditory hair cells, actin is found in the stereocilia, the cuticular plate and a circum-apical ring of filaments (Flock and Cheung, 1977; Flock et al., 1981; Tilney et al., 1980; Hirokawa and Tilney, 1982; Slepecky and Chamberlain, 1982, 1983, 1985, 1986). These networks contain different cross-linking proteins (Drenckhahn et al., 1991). Mammalian outer hair cells (OHCs) contain, in addition, an F-actin cortical lattice that lies between the plasma lemma and the layers of sub-surface cisternae (Flock et al., 1986; Bannister et al., 1988; Holley and Ashmore, 1988, 1990). In guinea-pig OHCs at least, there is also an actin-rich infracuticular network (Carlisle et al., 1988).

The β-actin isoform is known to be involved in dynamic maintenance of the hair bundle in rodents (Schneider et al., 2002; Rzadzinska et al., 2004). In chick, Hofer et al. (1997) reported that β-actin occurs in the stereocilia but not the cuticular plate, whereas γ-actin occurs in both, and suggested that the ratio of β:γ determines the final size and length of stereocilia. In mammals, decreasing stereociliary length (see e.g. Lim, 1986) and increasing stiffness of the hair bundles (Flock and Strelioff, 1984) towards the cochlear base might reflect changes in the ratio. The possibility that this ratio influences the structure and function of subcellular regions in other cell types makes it worth examining isoform distribution in mammalian hair cells and supporting cells in detail. We have therefore investigated the distribution of each isoform in different cell types and in two different frequency regions in the organ of Corti of guinea pig using post-embedding immunogold labelling.

2. Materials and methods

2.1. Animals and antibodies

Adult pigmented guinea pigs (500–850 g) exhibiting Preyer reflexes were killed with an overdose of sodium pentobarbitone (Vetalar®; 200 mg/kg IP), the bullae removed and opened. Cochleae were immediately perfused with, and immersed in, fixative for 2 h at room temperature and washed in phosphate buffered saline (PBS, pH 7.4). Subsequent processing varied according to the immunolabelling method. Animals were maintained and used in accordance with the "Principles of laboratory animal care" (NIH publication no. 85-23, revised 1985) and the UK Animals (Scientific Procedures) Act, 1986.

A mouse monoclonal IgG1 anti-β-actin antibody (clone AC-15, Product no. A-5441, Sigma-Aldrich, Dorset, UK) that recognises β-actin exclusively (Gimona et al., 1994) was used. A rabbit polyclonal antibody to γ-actin that does not cross react with β-actin (Otey et al., 1987) was the kind gift of Dr JC Bulinski. The latter antibody, which has been used in the chick (Hofer et al., 1997) and mammalian cochlea (Slepecky and Savage, 1994), was shown to be specific for cytoplasmic γ-actin in both.

2.2. Conventional transmission electron microscopy

Images from the cochleae of 10 normal animals were used for densitometric measurements and to illustrate the structures of interest. All cochleae were fixed in 2.5% glutaraldehyde in 0.1 M sodium cacodylate buffer, pH 7.4, for 2 h, followed by 1% osmium tetroxide in the same buffer for 1 h, dehydrated through an ethanol series and embedded in Spurr resin as described previously (Furness and Hackney, 1985). Ultrathin sections 100–120 nm thick were cut, stained in 2% uranyl acetate in 70% ethanol and 2% aqueous lead citrate and examined in JEOL 100CX or 1230 transmission electron microscopes (TEMs) operated at 100 kV. Images were acquired on Ilford TEM film or with a Megaview III digital camera and analySIS® software. The electron density of the filamentous structures was analysed using Adobe Photoshop® v.7.0 in negatives digitised with a Canon 9900F scanner with transparency adapter. The Autolevel function was first applied to the scanned images in order to reduce variability between pictures from different material. This function selects the brightest and darkest pixels in an image and makes them white and black, respectively. The intermediate pixels are then assigned grey level values proportionately resulting in a similar spread of grey levels in pictures of similar structural content. We then determined the mean pixel grey level of these regions using the Histogram function.

2.3. Immunofluorescence labelling

Two cochleae from two animals were fixed using 4% (w/v) freshly dissolved paraformaldehyde in 0.1 M sodium phosphate buffer (PB, pH 7.4). Cochlear spirals (modiolus and organ of Corti) were excised in PBS,

permeabilized in 0.1% (v/v) Triton-X-100 (30 min), incubated in 10% (v/v) goat serum in PBS (GS-PBS) blocking solution, and then in mixed anti-β-actin (diluted 1:200) and anti-γ-actin (diluted 1:400) in 1% (v/v) GS-PBS. After washing in 1% GS-PBS, spirals were incubated in FITC-conjugated goat anti-rabbit and TRITC-conjugated goat anti-mouse antibodies (diluted 1:50 in 1% GS-PBS) for 2 h, washed, dissected into segments which were mounted in 'antifade' (0.1% w/v *p*-phenylene diamine in 30% v/v glycerol and 1.5% w/v polyvinyl alcohol in PBS) and images were acquired using a X60/0.70 Nikon objective on a MRC1024 confocal microscope. Sequences of serial optical sections were obtained by consecutively changing the focal plane in 0.5 μm vertical steps. Images are presented either as single planes from the sequence or as a Z-stack made by superimposing all of the optical sections.

2.4. Post-embedding immunogold labelling

After fixation with 4% (w/v) freshly dissolved paraformaldehyde and 0.2% (v/v) glutaraldehyde in PB, the bony cochlear wall was partially removed and the cochleae dehydrated in 70%, 80% and 90% (10 min each) and 100% ethanol dried over molecular sieve (30 min) and immersed in LR-White resin (Agar Scientific Ltd., Stansted) for 16 h at room temperature. After several resin changes, they were placed in gelatin capsules filled with LR-White, capped to exclude air, and the resin polymerized at 50 °C for 24 h. After polymerisation, segments of the organ of Corti were obtained by microslicing (Jiang et al., 1993). In five cochleae, the length of organ of Corti was measured and distances from the apex corresponding approximately to the 0.5 kHz region (1 mm) and 5 kHz region (10 mm) selected according to the frequency map of Greenwood (1996). Ultrathin sections 120-nm thick were cut horizontally (parallel to the reticular lamina; $n = 2$) and radially ($n = 3$). To minimise differences in treatment, a ribbon of sections from one frequency location was collected onto one half of a 200-mesh thin bar nickel grid and, after drying, a ribbon from the second region collected on the other half.

Both single and double labelling were performed. Grids were incubated at room temperature (unless otherwise stated) in a moist chamber in small drops in the following sequence: 0.05 M Tris phosphate buffered saline (TBS, pH 7.4, 5 min); 10–20% (v/v) goat or bovine serum in TBS (STBS) for 30 min; primary antibody diluted 1:200–1:1000 in 1% STBS (either overnight at 4 °C or for 2 h at 37 °C); 1% STBS (10 min); 10–20% STBS (15 min); anti-mouse (for β-actin) or anti-rabbit (for γ-actin) secondary antibody conjugated to gold particles (British Biocell, UK), diluted 1:20 in 1% STBS (1 h). For double labelling, mixtures of both primary antibodies and both secondary antibodies with different sized particles (10 and 20 nm, or 5 and 10 nm) were used where appropriate. For negative controls, mouse ascites (mouse monoclonal, clone NS-1, Sigma) or rabbit IgG diluted to similar protein concentration were substituted for the primary antibody. After washing in distilled water, sections were dried briefly, stained with 2% aqueous uranyl acetate (20 min) and examined using TEM. Photographic plates (Ilford EM film) and digital images acquired with a Megaview II or III digital camera and analySIS® software, were obtained for analysis.

2.5. Semi-quantitative analysis

We analysed the apical actin-rich filamentous structures of the hair cells and supporting cells illustrated by conventional TEM in Fig. 1. To determine the relative density of labelling for each isoform in different cell types we analysed double-labelled sections of the two frequency regions from each animal collected on the same grid. Large gold particles were used for β-actin and small gold particles for γ-actin. Digital images were collected at a fixed magnification and particle density determined for each isoform. The areas of analysis varied because the relative size of each structure differed from section to section and between different structures.

The ratio of β- to γ-actin has been determined previously in a range of fibrocyte tissues in different species

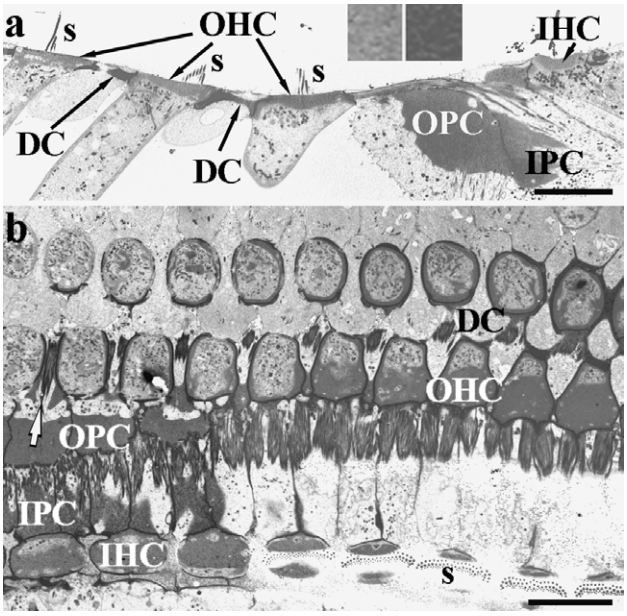

Fig. 1. (a) Radial TEM section illustrating cytoskeletal structures of the inner (IPC) and outer (OPC) pillar cell heads, Deiters' cell apex (DC) and the stereocilia (s) above the cuticular plates of IHCs and OHCs. The outer pillar cell head material appears denser than cuticular plate material. Scale bar = 10 μm. The two inset panels show 5× enlargements of equal areas of the row 2 OHC cuticular plate (left) and the OPC head (right) for direct comparison of their relative density. (b) Horizontal section at the level of the apical cytoskeletal networks. The first row of OHCs is separated from the IHCs by pillar cell apices, with a process from each outer pillar cell (arrow) separating adjacent OHCs. Abbreviations as for (a). Scale bar = 10 μm.

(Skalli et al., 1987). To estimate this ratio in cells of the organ of Corti from the relative labelling density, images were taken of type II fibrocytes in the cochlear wall in the same sections to determine the relative density of the labelling for each isoform.

Finally, qualitative observations suggested that monomeric filaments of each isoform were present. We assessed whether particles of one size were self-associated or randomly distributed amongst the other size of particles in images of outer pillar cells. To do this, we determined the proportion of each particle size and then, to account for possible aggregation, the proportion which had one or more of the same-sized particles within one particle width over an adjacent tissue-free area of resin. We then calculated the probability of random self-association of each particle size and the contributions of aggregation to obtain an expected frequency of association. We examined areas containing about 300 particles each in three pillar-cell images, and scored the particle size, together with the size of the nearest neighbour. The observed number in each category was compared with the predicted number using a χ^2 test.

3. Results

3.1. Immunofluorescence

Immunofluorescence labelling of whole mounts for confocal microscopy revealed differential distributions of the two isoforms of actin in hair cells and supporting cells (Fig. 2(a)–(e)) which could be compared with distributions observed by post-embedding immunogold (Fig. 2(f)–(h)). Labelling for β-actin was most prominent in the pillar-cell foot and head and at the ends of the phalangeal process of the outer pillar cell (Fig. 2(a)–(c)) but the centre of the head region was unlabelled (Fig. 2(c)). Within the cytoplasm of the outer pillar cell and Deiters' cell phalanges (Fig. 2(b)) and the OHC (Fig. 2(c)), the labelling was predominantly for γ-actin. Some areas showed strong colocalisation of both isoforms, in particular, the stereocilia and the actin associated with the microtubular bundles especially of both pillar cells and Deiters' cells (Fig. 2(a) and (c)). However, the colocalisation in the stereocilia was not homogenous. A sequence of three focal planes down through hair bundles showed apparently higher γ-actin labelling towards the tips of stereocilia, with colocalisation in the middle region and β-actin concentrated more at the base where the stereocilia insert into the cuticular plate (Fig. 3(a)).

3.2. Post-embedding immunogold labelling

With post-embedding immunogold, labelling could be seen which to some extent correlated with that observed by confocal microscopy but which also showed differences. Heavy labelling for β-actin could be seen throughout the head of the outer pillar cell (Fig. 2(f) and (h)), and in the phalangeal process (Fig. 2(f)). Heavy labelling for γ-actin was found over these locations, as well as on the cuticular plate of the hair cells which was difficult to detect by confocal microscopy (Fig. 2(g) and (h)). Exclusion of labelling from areas of high protein density has been noted previously in pre-embedding labelling for TEM (where the procedure is similar to immunofluorescence up to the point of visualisation) and is probably due to lack of penetration of antibodies into these regions (Mahendrasingam et al., 1998).

3.3. Hair cells

Gold labelling for β-actin was observed over the stereocilia and cuticular plates of both inner hair cells (IHCs – not shown) and OHCs (Fig. 3(b) and (c)). Labelling occurred throughout the cuticular plate but was particularly noticeable over the rootlets when they lay in the surface of the section (Fig. 3(b) and (d)), which is consistent with the fluorescence labelling showing greater β-actin towards the base (Fig. 3(a)).

In the shaft of the stereocilia, β-actin particles were found throughout the core but more frequently near the perimeter of the stereocilia (Fig. 3(c)). In order to determine whether this was a specific distribution, we compared the observed proportion of β-actin particles occurring peripherally versus that expected from a random distribution throughout the core. To be assigned to a 'peripheral' category, we chose to score particles that lie within one particle width (10 nm) of the boundary of the stereocilium. This is a conservative estimate because particles may lie up to ~25 nm from their target epitope (Matsubara et al., 1996). Thus, peripheral particles occupied a ring of 20 nm width with the stereocilium boundary as its centre, whereas all those inside this portion were assigned to a 'central' category (illustrated in the conventional TEM in Fig. 3(e)). Approximately 300 labelled profiles were assessed and all particles for β-actin placed into either the peripheral or central category.

By determining the relative areas of the ring and the total cross sectional area, based on an approximate diameter of 200 nm, we estimated that there was a 34% probability of the particles falling randomly in the peripheral ring. The counts showed, however, that 65% of the particles were peripheral and 35% central. The difference between the observed and predicted number of particles in each category was significant (χ^2 test with Yates' correction for one degree of freedom, $p > 0.001$). Thus the β-actin appears to be concentrated at the periphery of stereocilia. In conventional TEM, a zone of thicker dense filaments (diameter approx. 10 nm) can be observed in this region especially in the lower shaft of the stereocilia (Fig. 3(e) and (f)). These filaments

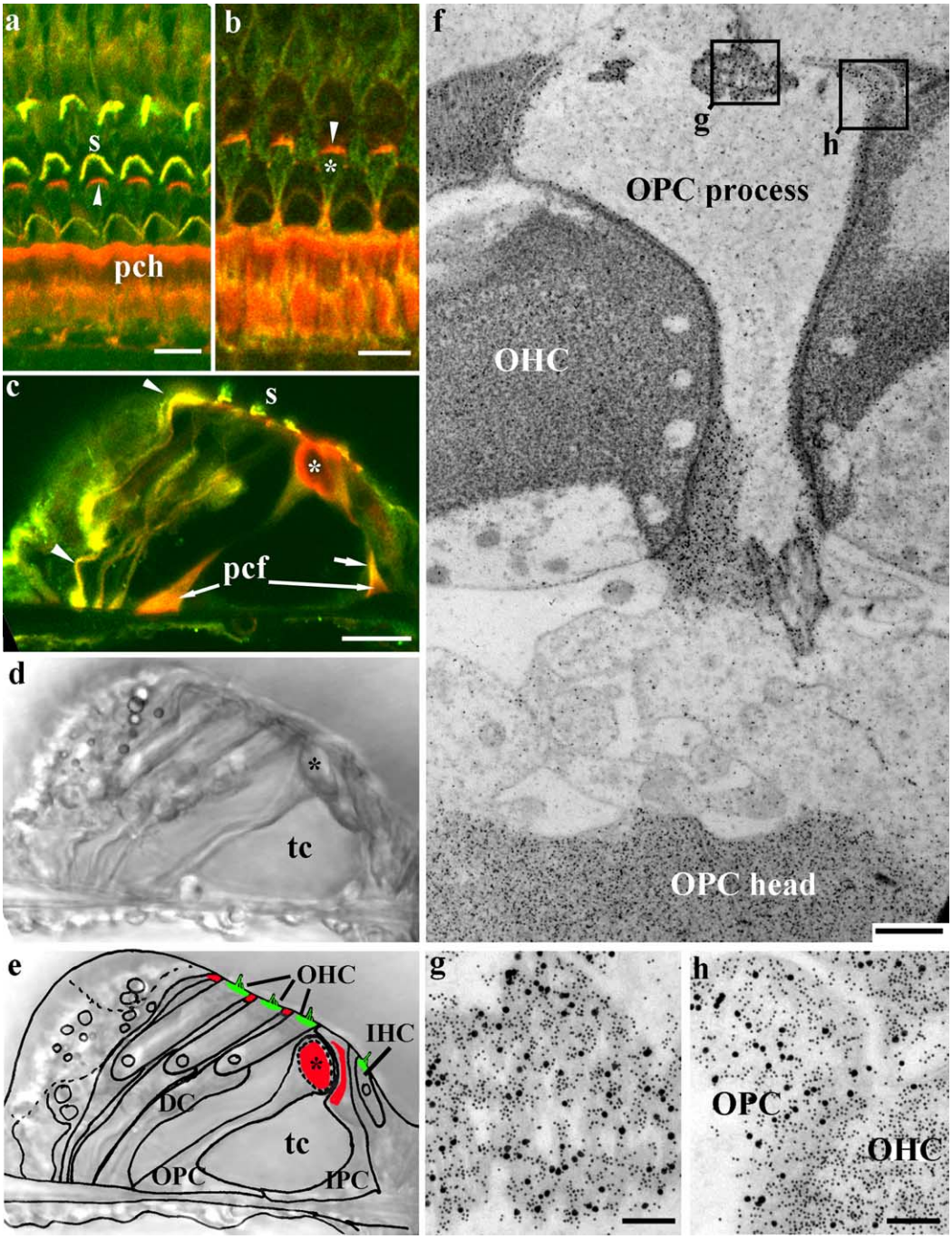

Fig. 2. (a–c) Confocal fluorescence images of an organ of Corti whole mount after double labelling for β-actin (red) and γ-actin (green); areas of colocalization appear yellow. (a) Horizontal Z-stack showing pillar cell heads (pch) and the end of the outer pillar cell process (arrowhead) rich in β-actin whilst stereocilia (s) show colocalisation. Scale bar = 10 μm. (b) Single image showing γ-actin in the cytoplasm of the outer pillar cell process (*) and β-actin at the end (arrowhead). Scale bar = 10 μm. (c) Radial view showing strong β-actin labelling in the pillar cell heads (*), and colocalization in pillar cell feet (pcf) and microtubule bundles (arrow), and Deiters' cell microtubule bundle (arrowheads). Scale bar = 20 μm. (d, e) Transmitted light micrograph of (c) and diagram superimposed on (d) to show the tunnel of Corti (tc), pillar cells (IPC, OPC) and their head region (*), Deiters' cells (DC), IHC and OHCs. Red areas define the Deiters' and pillar cell apices and green areas, the hair cell apices investigated semi-quantitatively by immunogold labelling. Scale as in (c). (f) Horizontal TEM section immunogold labelled for β- (large particles) and γ-actin (small particles). The outer pillar cell (OPC) head is rich in β-actin but the OHCs show less labelling; boxes indicate regions shown at higher magnification in (g) and (h). Scale bar = 1 μm. (g) The β-actin rich end of the outer pillar cell process also contains high levels of γ-actin. (h) Comparison showing weaker labelling of β-actin but high levels for γ-actin in the OHC compared with the outer pillar cell (OPC). Scale bars (g, h) = 200 nm. (For interpretation of the references to colour in this figure legend, the reader is referred to the web version of this article.)

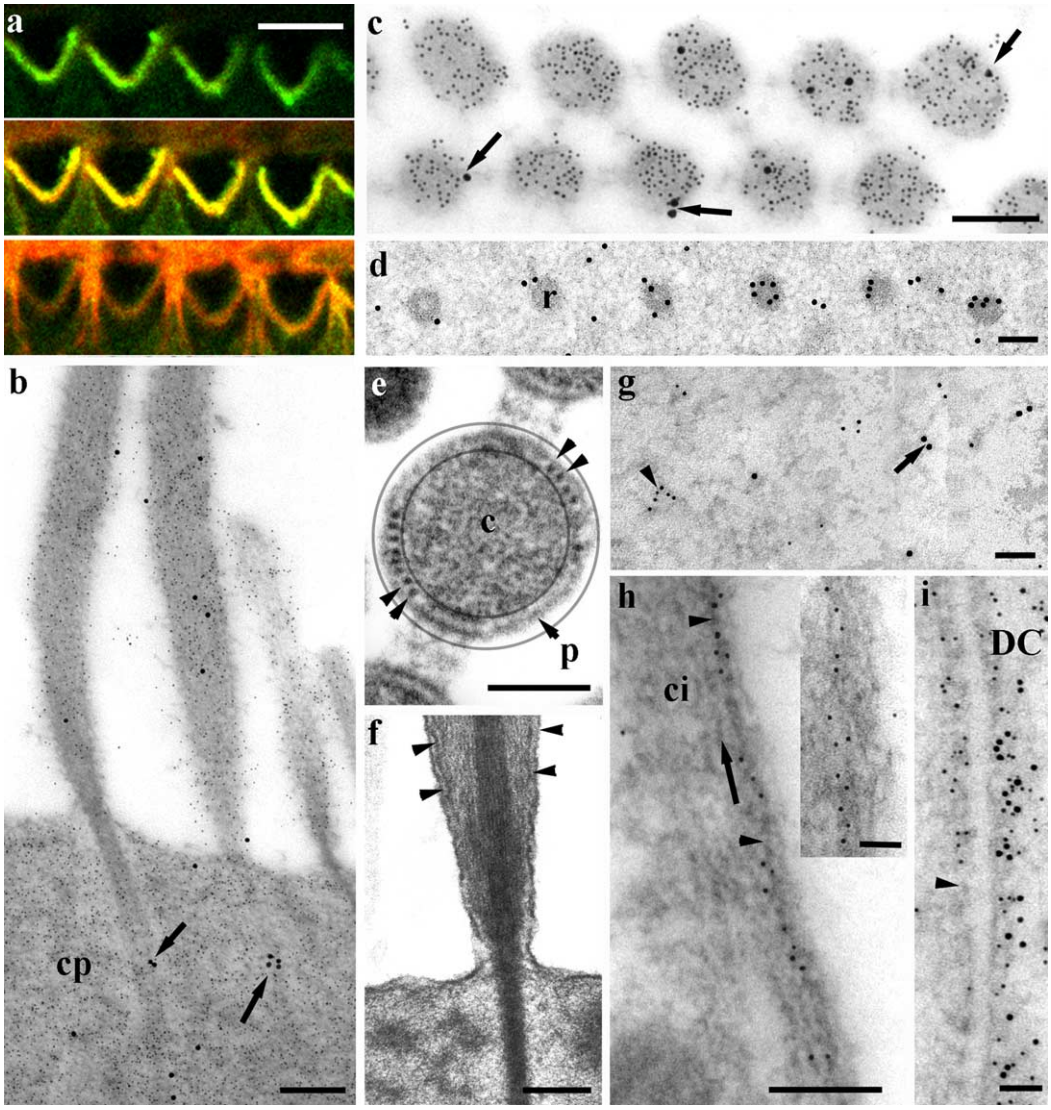

Fig. 3. (a) Sequential confocal images of four OHC stereociliary bundles separated by 0.5 μm steps in the *z*-direction after double labelling for β-actin (red) and γ-actin (green). Note that the upper image (towards the tips) appears green, i.e., representing predominantly γ-actin, the middle one, yellow, showing colocalisation, and the lower one, red, representing predominantly β-actin. Scale bar = 10 μm. (b) Radial TEM section of an OHC apex double immunogold labelled for β- (large particles) and γ-actin (small particles). Labelling for both γ- and β-actin occurs over the stereocilia and cuticular plate (cp) with β-actin labelling being particularly associated with the rootlets (arrows). Particles for β-actin appear to occur both peripherally and centrally in stereocilia. However, it is not possible to tell whether longitudinal sections, which are ~half the thickness of the stereocilia, also graze the periphery of the shaft and expose it to labelling in one or other surface of the section because it would be superimposed over the wider central region. Thus, apparently central labelling cannot be unambiguously distinguished from peripheral labelling in this plane of section. Scale bar = 200 nm. (c) In horizontal sections of stereocilia, there is equal access to the central core and the periphery for immunogold labelling. The majority of the labelling for β-actin is peripheral (e.g., arrows), but there are also some central particles. The labelling for γ-actin is more uniformly distributed. Scale bar = 200 nm. (d) Horizontal sections single labelled for β-actin show labelling of rootlets (r). Scale bar = 100 nm. (e) Conventional TEM showing thicker filaments (arrowheads) in the periphery (p) compared with the core (c). Scale bar = 100 nm. (f) Longitudinal section showing peripheral thick filaments (arrowheads). Scale bar = 100 nm. (g) OHC cytoplasm showing sparse labelling for both isoforms. Gold particles of the same sizes (small – arrowhead; large – arrow) tend to associate with each other. Scale bar = 100 nm. (h) Lateral wall of a double labelled OHC showing only γ-actin associated with the dense band (arrowheads) between the outermost layer (arrow) of cisternae (ci) and the plasma membrane. Scale bar = 150 nm. Inset: Tangential view of the lateral wall showing a clear line of γ-actin particles in the region of the filamentous cortical lattice beneath the plasma membrane. Scale bar = 50 nm. (i) Region of the lateral wall below the nucleus and next to the Deiters' cell (DC) cup. Note the labelling for γ-actin becomes very sparse after the lattice terminates (arrowhead). Scale bar = 100 nm. (For interpretation of the references to colour in this figure legend, the reader is referred to the web version of this article.)

appear to be distinct from the central core of actin filaments and also from an area of enhanced density associated with the anchoring of the lateral links between adjacent stereocilia (Fig. 3(e)). There was sparse labelling over the cytoplasm of the hair cells for β-actin (Fig. 3(g)).

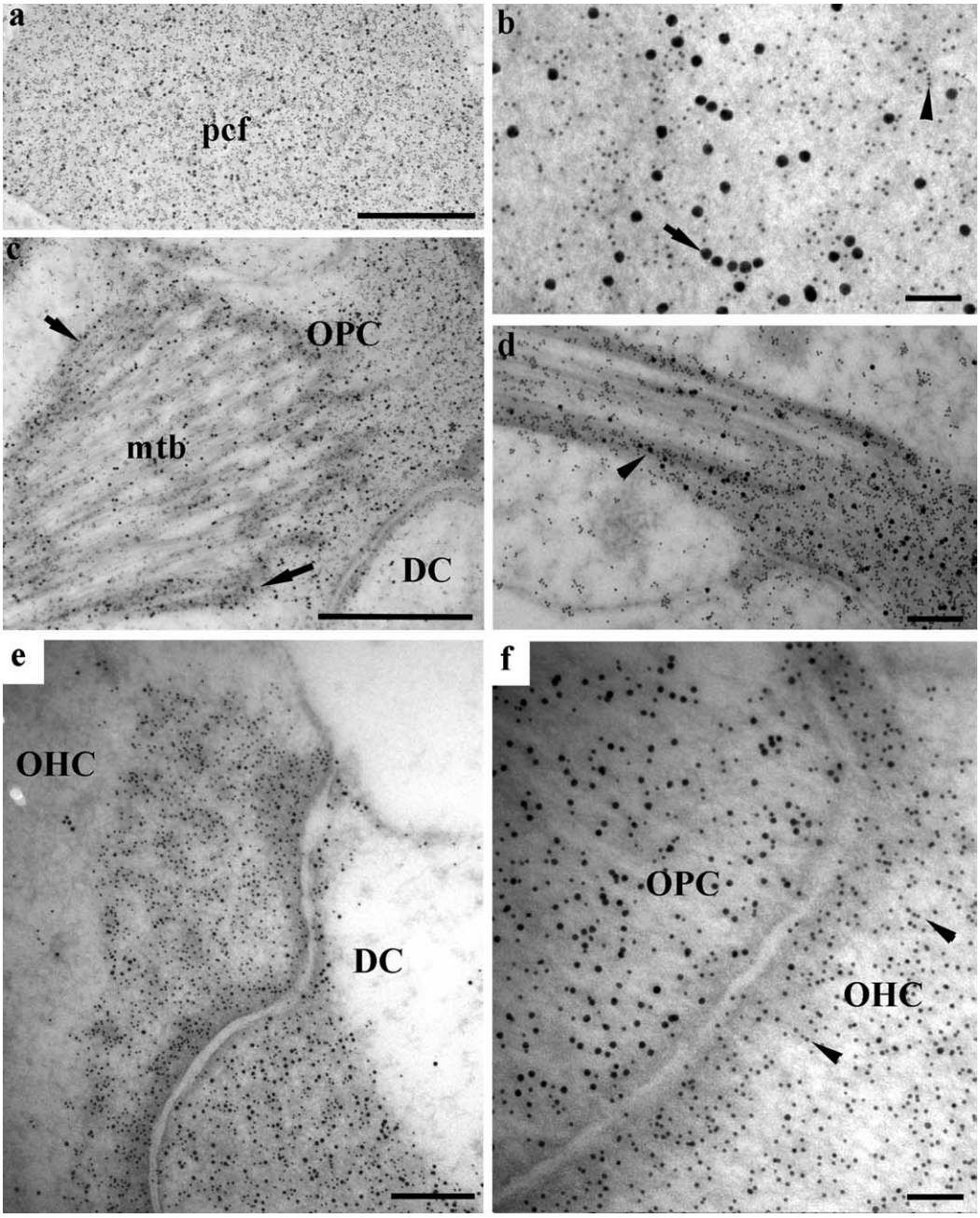

Fig. 4. Post-embedding double labelling in supporting cells. (a) Outer pillar cell foot (pcf) showing dense labelling for both isoforms. Scale bar = 1 μm. (b) Central portion of an outer pillar cell head showing particles of both sizes forming lines and groups consisting of one size or the other (e.g., arrows; arrowheads). Scale bar = 50 nm. (c) Horizontal section of Deiters' cell (DC), and outer pillar cell (OPC) apices. Labelling for γ-actin occurs throughout the pillar cell microtubule bundle (mtb) whilst that for β-actin is denser at the edges (e.g., arrows). Scale bar = 750 nm. (d) Radial section of a Deiters' cell. Labelling for both isoforms is stronger at the edge of the microtubule bundle (arrow) but also occurs within it. Scale bar = 200 nm. (e) Radial section of Deiters' cell (DC) and OHC junction; there is dense labelling for β- and γ-actin in the DC, whereas γ-actin predominates in the hair-cell cuticular plate. Scale bar = 200 nm. (f) Radial section of an OHC and outer pillar cell (OPC) junction. Labelled filaments are oriented towards the junction (e.g., arrowheads). Scale bar = 100 nm.

Gold labelling for γ-actin was present over the stereocilia and cuticular plate (Fig. 3(b) and (c)). The distribution throughout these structures appeared to be fairly homogeneous. Labelling was also found to be present throughout the cytoplasm (Fig. 3(g)) but was particularly associated with the lateral wall of the OHCs (Fig. 3(h)) and IHCs (not shown). This lateral wall labelling occupied a distinct region closer to the plasma membrane compared with the nearby labelling for β-actin which was deeper within the cell, and became sparse where the cortical lattice terminates below the region of the nucleus (Fig. 3(i)).

3.4. Supporting cells

In both inner and outer pillar cells, a much higher density of β-actin gold particles was seen over the filamentous plates of the head and foot regions compared with the cuticular plate and stereocilia of hair cells (Figs. 3(b), 4). The centre of the head plate was heavily labelled (Fig. 4(b)). Labelling was also prominent alongside the outer margins of the microtubule bundles of the pillar cells and on the anchoring filaments at their ends, and to a lesser extent within the bundles (Fig. 4(c)).

Labelling for γ-actin was noted in the same locations (Fig 4(a)–(c)). However, the difference in density of particles between hair-cell and supporting-cell apical cytoskeletal structures appeared qualitatively to be less than the differences in density of labelling for β-actin in these two areas, suggesting differences in the relative distribution of the two.

In Deiters' cells, labelling for both β- and γ-actin was strongly present over the dense material adjacent to the apical junctional complex (Fig. 4(d) and (e)), along the microtubule bundles (Fig. 4(d)) and over the 'cup' region enclosing the base of the OHC. β-actin was especially enriched adjacent to the plasma membrane of the cup abutting the OHC (Figs. 3(i), 5). Dense labelling for both isoforms was also seen over the filamentous structures adjacent to the junctions in border cells and inner phalangeal cells (data not shown).

3.5. Innervation

Both afferent and efferent nerve endings onto IHC and OHC bases labelled for β-actin (Fig. 5). In the afferent endings, gold particles were found predominantly along the inner side of the plasma membrane facing the hair cells, whilst in the efferent endings labelling was found over the cytoplasm and was particularly concentrated along the lateral membranes. There was little labelling on the hair-cell side of the synaptic regions. Labelling for γ-actin was found over both terminal types but no consistent pattern was detected (not shown).

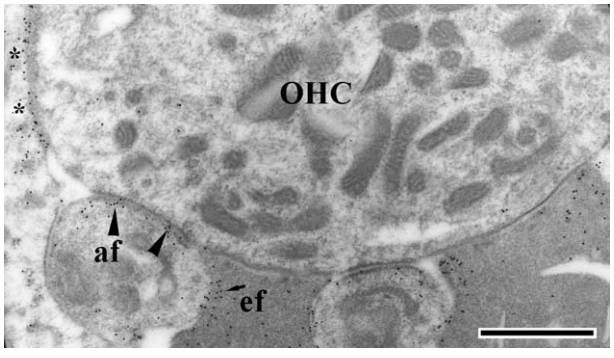

Fig. 5. Single labelling for β-actin over the synaptic region of an OHC. In the efferent (ef), labelling occurs over the lateral margins (arrow), whilst in the afferent (af), labelling occurs alongside the membrane abutting the hair cell (arrowheads). Labelling is also concentrated near the membrane of the Deiters' cell cup (*) around the OHC. Scale bar = 1 μm.

3.6. Semi-quantitative analysis

It cannot be assumed that the two antibodies label their respective antigens with equal efficiency so it is not possible to compare directly the densities of labelling for the two isoforms without calibrating their relative ability to label the target (see later). Thus we have primarily compared labelling density in different structures separately for each isoform. We also compared two different cochlear regions, the 0.5 and 5 kHz-regions.

Counts of gold particles for β-actin confirmed that the supporting-cell cytoskeletal structures were labelled very strongly compared to the hair-cell cuticular plate

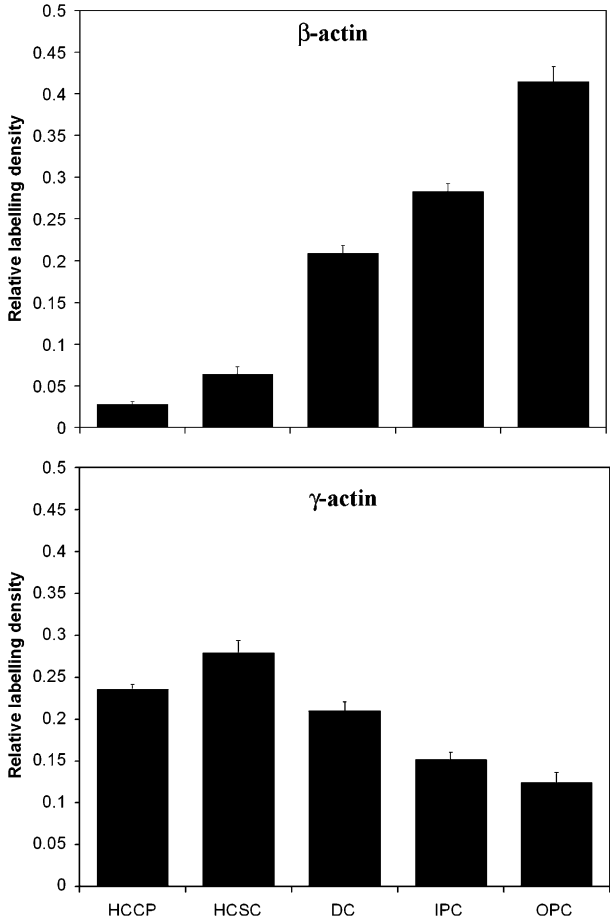

Fig. 6. Mean proportional labelling densities of γ-actin and β-actin in cells of the organ of Corti. Data obtained from 7 different groups of sections (5 from the 0.5 kHz-region and 2 from the 5-kHz region) from 5 animals. Groups were excluded if some cell types were not represented. Note high levels of β-actin in supporting cells compared with hair cells, and the almost converse relationship for γ-actin. However, both isoforms are more concentrated in the stereocilia than the cuticular plate. Data for hair cells are derived from both IHCs and OHCs. HCCP = hair cell cuticular plate; HCSC = hair cell stereocilia; DC = Deiters' cell; IPC = inner pillar cell; OPC = outer pillar cell.

Table 1
Comparison of labelling densities between different cell types for each isoform

Cell structure	Relative β-actin density	Relative γ-actin density
HCCP	1	1
HCSC	2.57	1.1
DC apex	10.71	0.86
IPC head	11.37	0.67
OPC head	19.36	0.44

Relative β-actin or γ-actin labelling density is expressed with respect to the cuticular plate/apical region in both cases. The labelling density for β-actin in outer pillar cells is 20-fold that in the hair cells, with the other cells in between. The differences in relative density of γ-actin between cells are much smaller. HCCP = OHC cuticular plate; HCSC = hair cell stereocilia; DC = Deiters' cell; IPC = inner pillar cell; OPC = outer pillar cell.

and stereocilia. The mean relative labelling density determined from at least three cell profiles per region per animal decreased in the following order: outer pillar cells > inner pillar cells > Deiters' cells > hair cells (Fig. 6). In the hair cells, the density of labelling for β-actin was higher in the stereocilia than in the cuticular plate. The overall amounts are summarised in Table 1, relative to the density of labelling for each isoform in the hair-cell cuticular plate. Thus, outer pillar cell heads had almost 20-fold higher labelling than the cuticular plate of hair cells for β-actin and inner pillar cells and Deiters' cells over 10-fold. The stereocilia were about 2.5-fold more heavily labelled than the cuticular plate overall.

In comparison, labelling density for γ-actin showed almost the converse pattern, but relative differences were smaller than for β-actin (Fig. 6). Thus, hair-cell cuticular plates were about 2-fold more densely labelled than outer pillar cell heads, with the other cells in between (Table 1). The only exception to this reversal of pattern compared with that for β-actin was that labelling for γ-actin in the stereocilia was marginally higher than in the cuticular plate, but only by about 1.1-fold, i.e., less than the difference observed for β-actin.

The only consistent difference detected between the 0.5- and 5-kHz frequency regions was in the outer pillar cells which showed a decrease in the 5-kHz region in γ-actin labelling, overall by 1.4-fold and an increase in the β-actin of 1.5-fold (Fig. 7). These differences were significant (median test, $p < 0.01$). Whilst the mean relative labelling of the cuticular plate of OHCs appeared to be higher for β-actin in the 0.5-kHz region, a significant difference was not detected.

3.7. Ratios of β- to γ-actin

Some sections also had portions of the cochlear lateral wall which contains fibrocytes. Fibroblastic tissues from different sources such as cornea and endometrium in rats and humans always contain more β-actin than γ-actin, on average about 2.6:1 β:γ (range from 2.5 to 4.2; Skalli et al., 1987). Thus, we assumed a similar ratio of β:γ in cochlear fibrocytes in order to calibrate the labelling density for the two isoforms. In 10 random pictures of fibrocytes from one section, the mean β:γ labelling density was 1:22, which when adjusted for the predicted ratio, indicates that the γ-actin antibody labels 60× more heavily than the β-actin antibody on this section. We used this measure of relative binding to estimate the ratio of β:γ in the hair cells and supporting cells in the same section.

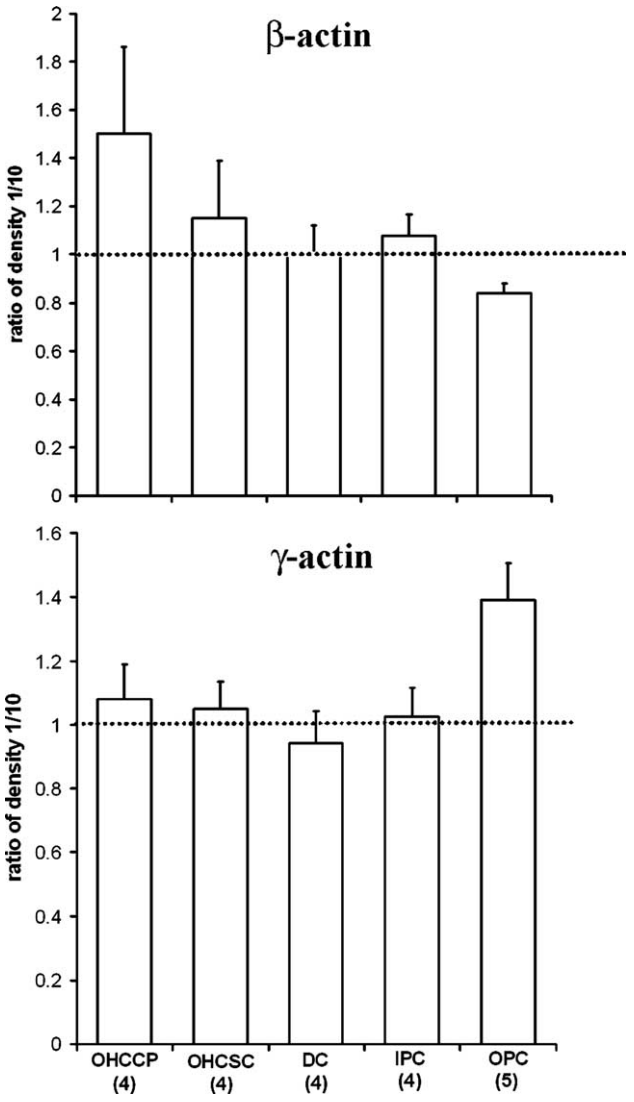

Fig. 7. Graphs comparing labelling in different frequency regions expressed as ratios (i.e., density in the 0.5-kHz [1 mm] divided by density in 5-kHz [10 mm] region). The number of samples is given in brackets. IHCs have been omitted from this comparison because of small numbers. Consistent differences only occurred in outer pillar cells which showed higher labelling for β-actin and lower labelling for γ-actin in the 5-kHz region (ratios significantly different from 1; median test, $p > 0.01$). The variance in the stereociliary and cuticular plate labelling for β-actin was high. OHCCP = OHC cuticular plate; OHCSC = OHC stereocilia; DC = Deiters' cell; IPC = inner pillar cell; OPC = outer pillar cell.

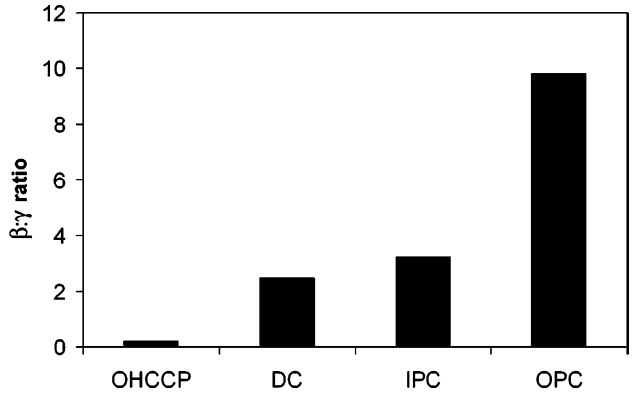

Fig. 8. Histogram illustrating the ratio of β:γ labelling density after the adjusting values according to the relative affinity of the two antibodies for their respective antigens under these tissue preparation conditions. Their relative affinity was determined from labelling densities in fibrocytes where the β:γ ratio has been obtained in other studies. After adjustment, the β:γ ratio appears to be highest in outer pillar cells and lowest in hair cells.

The estimated β:γ ratio is illustrated in Fig. 8. These values suggest that there is a considerable difference between hair cells and supporting cells. Thus the β:γ ratio for a hair-cell cuticular plate is in the order of 1:5, whilst the β:γ ratio for an outer pillar cell head is around 10:1. However, because there is more enrichment of β-actin (2.5-fold) in stereocilia compared with the cuticular plate than is the case for γ-actin (1.1-fold); the β:γ ratio there may be about 1:2.

We noticed that in conventional TEMs, the outer pillar cell head in particular appeared to be denser than cuticular plates (Fig. 1). To confirm this, we measured the grey levels (electron density) of these regions in digitised images. The mean grey level of the OHC cuticular plate was 90% ± 4% (mean ± SD) that of the outer pillar cell head.

3.8. Monomeric filaments

In pillar and Deiters' cells apices, where particles for both β-actin and γ-actin were well represented, there were chains of particles of the same size (Fig. 4(b)). Often particles formed parallel rows which may represent groups of parallel filaments (Fig. 4(f)). In the lateral wall of the OHCs, there was virtually no coincidence between labelling for β- or γ-actin (Fig. 3(h) and (i)). In the hair-cell cytoplasm, particles representing both isoforms were rarely associated with each other, instead tending to associate preferentially with particles of the same size (Fig. 3(g)). We therefore investigated the possibility that there were homomeric filaments in cells of the organ of Corti.

We analysed images of labelled pillar-cell apices to determine whether adjacent particles were randomly associated or segregated to some degree into the two sizes. We also assessed aggregation over nearby tissue-free resin. The densities and therefore probabilities, varied for each image, because they came from different experiments, but in one example, 60% of particles represented β-actin. Thus, the probability of two β-actin particles self-associating was $0.6 \times 0.6 = 0.36$ (36%) with aggregation accounting for a further 5% (total 41%); however, the observed association of β-actin particles was 50%. The probability of two γ-actin particles associating was $0.4 \times 0.4 = 0.16$ (16%) with an additional 1% contribution from aggregation (total 17%) whilst the observed association was 36%. The probability of the two different particles sizes associating is $100 - (41 + 17) = 42\%$, whilst the observed value was 24%. The differences between observed and expected values for all three images were significant (χ^2 test, $p > 0.01$). Thus, the self-association of particles suggested that the isoforms are not randomly distributed but are self-associated.

3.9. Control sections

When either rabbit IgG or mouse ascites fluid was substituted for the primary antibody, there was virtually no labelling (not shown).

4. Discussion

4.1. Post-embedding immunogold assessment of actin isoform distributions

We describe here relative distributions of β- and γ-actin isoforms in hair cells and supporting cells in the guinea-pig organ of Corti, thus extending previous immunocytochemical studies by Slepecky and Savage (1994) and Hofer et al. (1997). The semi-quantitative data were derived from immunogold labelling densities in equivalent cochlear regions from 5 animals. Consistent relative differences between cell types were found in all samples, even though comparative labelling densities for the two isoforms varied, probably due to differences in experimental conditions in different labelling runs.

Our results show that there is more β-actin but less γ-actin in supporting cells relative to hair cells and that there is more β-actin and less γ-actin in outer pillar cells from a high frequency than a low frequency location. We also found isoform ratios of 1:5 β:γ in stereocilia and 1:2 in the cuticular plate of hair cells, similar to the ratio obtained in chick from Western blots of 1:2 β:γ (Hofer et al., 1997). In contrast, the pillar cell apical plate may contain 10:1 β:γ; the latter has greater electron density than hair-cell cuticular plates suggesting a higher filament density and/or a different constellation of actin-associated proteins.

The two isoforms also appear to form homomeric filaments or to at least form regions of filament composed of one isoform. This has not been shown previously, to our

knowledge, and together with other aspects of isoform sorting implies that the isoforms may be spatially independently regulated.

4.2. Sorting of the actin isoforms

One suggested mechanism for sorting is that each isoform interacts preferentially with particular associated proteins, themselves distributed differentially (Hofer et al., 1997). One protein that displays a similar distribution to γ-actin in the organ of Corti is spectrin. Spectrin is found in supporting cells (Mahendrasingam et al., 1998) and in hair cells in the cuticular plate (Slepecky and Ulfendahl, 1992) and stereocilia (Zine and Romand, 1993, Mahendrasingam et al., 1998), and it cross links actin flaments in the OHC lateral wall (Holley and Ashmore, 1988, 1990). The smaller relative difference in γ-actin between supporting cells and hair cells compared with β-actin and its predominance in similar locations to spectrin is consistent with such an association.

Cytoplasmic actins are also known to interact with the plastin-fimbrin family (Prassler et al., 1997) and I-plastin is present in the cuticular plate and stereocilia of hair cells where it presumably cross-links actin filaments (Daudet and Lebart, 2002). Another actin cross-linker, espin, appears to be confined to stereocilia (Loomis et al., 2003). The latter may thus associate selectively with β-actin within hair cells.

The peripheral localisation of β-actin in stereociliary shaft and its predominance in the rootlets is of interest because it could represent localised sorting of the isoforms in the actin bundle. This peripheral localisation was not reported in the developing rat cochlea by Schneider et al. (2002) nor by Rzadzinska et al. (2004). However, it only became apparent to us in adult guinea pigs when we cut and labelled transverse sections of the stereocilia towards their bases. Neither γ-actin antibodies nor secondary antibodies alone preferentially labelled the periphery so this distribution seems unlikely to be a fixation artefact. However, one possibility is that cross-linking proteins in the core might mask or alter the epitopic site recognised by the β-actin antibody and thereby inhibit labelling over the centre. Alternatively, β-actin may indeed be specifically associated with proteins found in the periphery and rootlets. Peripheral proteins include myosin VIIa, myosin 1c (Garcia et al., 1998) and myosin-associated proteins such as harmonin, vezatin and whirlin (see review by Frolenkov et al., 2004). Myosin VI (Hasson et al., 1997) and radixin (Pataky et al., 2004), a member of the ERM family of proteins, occur towards the ankle/taper region. Our sequential confocal images suggest that β-actin is more prominent in the lower part of the stereocilia, thus potentially colocalising with the radixin. In fact, in epithelial cells of rabbit gastric glands, labelling near the apical membrane suggests that β-actin interacts with ezrin (Yao et al., 1995) which has homology to radixin (Sato et al., 1992). Radixin may thus play an analogous role in linking β-actin to the membrane.

We observed marginally thicker, dense filaments in the periphery of the stereociliary shaft by conventional TEM. This denser appearance could reflect a higher β-actin content, compared with central filaments. Purified actin isoforms form structurally different filaments (Allen et al., 1996) implying that they could also appear different in TEM. Alternatively, the denser appearance of the peripheral filaments could be a result of other proteins being linked to them that do not occur in the centre of the stereocilia.

The relatively high levels of β-actin in supporting cells suggest the latter may contain unique features that influence actin localisation; for example, myosin 1b has been reported to be exclusive to supporting cells (Dumont et al., 2002). However, levels of β-actin expression correspond most notably with the quantity of microtubules in the supporting-cell bundles, i.e., it is greatest in outer pillar cells and increases towards the cochlear base as do the number of microtubules (Kikuchi et al., 1991). Labelling for β-actin was clearly associated with the microtubule bundles in the supporting cells and with the electron-dense regions in which they terminate. Pillar and Deiters' cell microtubules are unusual, containing 15 protofilaments as compared with hair-cell microtubules which, like most others, have 13. They may thus have unique features that enable them to interact preferentially with β-actin. It is furthermore possible that microtubule associated proteins (MAPs) influence actin distributions; for example, it is known that MAP1b and MAP2 have actin binding domains (see review by Dehmelt and Halpain, 2004). A 205 kDa MAP is present in both hair cells and supporting cells (Oshima et al., 1992), although so far no interaction with actin has been reported.

4.3. Functional differences between actin isoforms

Despite the considerable sequence similarity (see review by Khaitlina, 2001), β- and γ-actin may confer different properties on hair cells and supporting cells. In other tissues (see e.g. Erba et al., 1988), differences in distribution, interaction with binding proteins and developmental time course of expression imply distinct functional roles, with β-actin found in more dynamic regions, whilst γ-actin is associated with more stable regions of the cell (Micheva et al., 1998).

The observations made by Schneider et al. (2002) in early postnatal rodent cochlear organ culture show that β-actin is incorporated into the stereocilium tip and travels down the shaft at the rate of 2.5 μm per day. This indicates a relatively dynamic expression at least during development that might be modulated to effect repair or to confer greater resistance to damage in adulthood. Indeed, relatively long duration sound stimulation apparently alters F-actin expression in the adult organ of Corti (Hu and Henderson, 1997).

It is also possible that differences in isoform composition influence the mechanical properties of the cells. OHC motility is thought to be based on prestin (Zheng et al., 2000), a basolateral plasma membrane molecule that changes conformation with changes in membrane potential. The cortical lattice that underlies the plasma membrane, which predominantly contains γ-actin, probably helps to convey these motile forces to the cell as a whole (Holley and Ashmore, 1988, 1990). If γ-actin is crucial to the prestin-driven length changes that underlies the role of these cells in cochlear amplification (Zheng et al., 2000), this may explain the nonsyndromic hearing loss that occurs when the gene for it is mutated (Wijk et al., 2003).

The supporting cell microtubule bundles are embedded at either end in plates (Kikuchi et al., 1991; Henderson et al., 1995) which our data suggest are enriched in β-actin. Biophysical measurements indicate that the pillar cells are structures of particular stiffness. They have an axial stiffness 3 to 4 orders of magnitude greater than OHCs (Tolomeo and Holley, 1997a,b), primarily due to the microtubule bundle. The maximum linear stiffness of the basilar membrane measured between the radial anchoring points occurs under the outer pillar cells, suggesting that they may contribute more to its stiffness than other cells (Olson and Mountain, 1994; Emadi et al., 2004) and the basilar membrane itself becomes stiffer towards the base. It is possible that β-actin expression increases where greater anchoring or stiffening of structures is required in the organ of Corti, presumably to anchor the microtubular bundle which enables them to act as supporting or stiffening elements. Consistent with this, gels composed only of β-actin are apparently very inelastic compared with the other isoforms so far measured (Allen et al., 1996), although their study did not examine cytoplasmic γ-actin. However, systematic measurements of the stiffness or strength of the apical structures enriched in the different isoforms in the organ of Corti are not yet available. Thus, to deduce the respective roles of these isoforms in the cochlea requires further investigation of their specific associations with other proteins and the biophysical properties of the different cell types.

Acknowledgements

Supported by the Wellcome Trust, Defeating Deafness and Tohoku University Hospital. We thank Mr. S. Murray and Mrs. K. Walker for technical assistance, and Dr. J. Bulinski for the γ-actin antibody.

References

Allen, P.G., Shuster, C.B., Kas, J., Chaponnier, C., Janmey, P.A., Herman, I.M., 1996. Phalloidin binding and rheological differences among actin isoforms. Biochemistry 35, 14062–14069.

Bannister, L.H., Dodson, H.C., Astbury, A.R., Douek, E.E., 1988. The cortical lattice: a highly ordered system of subsurface filaments in guinea pig cochlear outer hair cells. Prog. Brain Res. 74, 213–219.

Carlisle, L., Zajic, G., Altschuler, R.A., Schacht, J., Thorne, P.R., 1988. Species differences in the distribution of infracuticular F-actin in outer hair cells of the cochlea. Hearing Res. 33, 201–206.

Daudet, N., Lebart, M.C., 2002. Transient expression of the t-isoform of plastins/fimbrin in the stereocilia of developing auditory hair cells. Cell Motil. Cytoskel. 53, 326–336.

Dehmelt, L., Halpain, S., 2004. Actin and microtubules in neurite initiation: are MAPs the missing link? J. Neurobiol. 58, 18–33.

Drenckhahn, D., Engel, K., Hofer, D., Merte, C., Tilney, L., Tilney, M., 1991. Three different actin filament assemblies occur in every hair cell: Each contains a specific actin crosslinking protein. J. Cell Biol. 112, 641–651.

Dumont, R.A., Zhao, Y.D., Holt, J.R., Bahler, M., Gillespie, P.G., 2002. Myosin-I isozymes in neonatal rodent auditory and vestibular epithelia. J. Assoc. Res. Otolaryngol. 3, 375–389.

Emadi, G., Richter, C.P., Dallos, P., 2004. Stiffness of the gerbil basilar membrane: radial and longitudinal variations. J. Neurophysiol. 91, 474–488.

Erba, H.P., Eddy, R., Shows, T., Kedes, L., Gunning, P., 1988. Structure, chromosome location, and expression of the human gamma-actin gene: differential evolution, location, and expression of the cytoskeletal beta- and gamma-actin genes. Mol. Cell Biol. 8, 1775–1789.

Flock, Å, Cheung, H.C., 1977. Actin filaments in sensory hairs of inner ear receptor cells. J. Cell Biol. 75, 339–343.

Flock, Å, Strelioff, D., 1984. Graded and nonlinear mechanical properties of sensory hairs in the mammalian hearing organ. Nature 310, 597–599.

Flock, Å, Flock, B., Ulfendahl, M., 1986. Mechanisms of movement in outer hair cells and a possible structural basis. Arch. Otorhinolaryngol. 243, 83–90.

Flock, Å, Cheung, H.C., Flock, B., Utter, G., 1981. Three sets of actin filaments in sensory cells of the inner ear. Identification and functional orientation determined by gel electrophoresis, immunofluorescence and electron microscopy. J. Neurocytol. 10, 133–147.

Frolenkov, G.I., Belyantseva, I.A., Friedmann, T.B., Griffith, A.J., 2004. Genetic insights into the morphogenesis of inner ear hair cells. Nature Rev. Gen. 5, 489–498.

Furness, D.N., Hackney, C.M., 1985. Cross-links between stereocilia in the guinea pig cochlea. Hearing Res. 18, 177–188.

Garcia, J.A., Yee, A.G., Gillespie, P.G., Corey, D.P., 1998. Localization of myosin-Ibeta near both ends of tip links in frog saccular hair cells. J. Neurosci. 18, 8637–8647.

Gimona, M., Vandekerckhove, J., Goethals, M., Herzog, M., Lando, Z., Small, J.V., 1994. β-Actin specific monoclonal antibody. Cell Motil. Cytoskel. 27, 108–116.

Greenwood, D.D., 1996. Comparing octaves, frequency ranges, and cochlear-map curvature across species. Hearing Res. 94, 157–162.

Hasson, T., Gillespie, P.G., Garcia, J.A., MacDonald, R.B., Zhao, Y., Yee, A.G., Mooseker, M.S., Corey, DP., 1997. Unconventional myosins in inner-ear sensory epithelia. J. Cell Biol. 137, 1287–1307.

Henderson, C.G., Tucker, J.B., Mogensen, M.M., Mackie, J.B., Chaplin, M.A., Slepecky, N.B., Leckie, L.M., 1995. Three microtubule-organizing centers collaborate in a mouse cochlear epithelial-cell during supracellularly coordinated control of microtubule positioning. J. Cell Sci. 108, 37–50.

Herman, I.M., 1993. Actin isoforms. Curr. Opin. Cell Biol. 5, 48–55.

Hirokawa, N., Tilney, L.G., 1982. Interactions between actin filaments and membranes in quick-frozen and deeply etched hair cells of the chick ear. J. Cell Biol. 95, 249–261.

Hofer, D., Ness, W., Drenckhahn, D., 1997. Sorting of actin isoforms in chicken auditory hair cells. J. Cell Sci. 110, 765–770.

Holley, M.C., Ashmore, J.F., 1988. A cytoskeletal spring in cochlear outer hair cells. Nature 335, 635–637.

Holley, M.C., Ashmore, J.F., 1990. Spectrin, actin and the structure of the cortical lattice in mammalian cochlear outer hair cells. J. Cell Sci. 96, 283–291.

Hu, B.H., Henderson, D., 1997. Changes in F-actin labelling in the outer hair cell and the Deiters' cell in the chinchilla cochlea following noise exposure. Hearing Res. 110, 209–218.

Jiang, D., Furness, D.N., Hackney, C.M., Lopez, D.E., 1993. Microslicing of the resin-embedded cochlea in comparison with the surface preparation technique for analysis of hair cell number and morphology. Brit. J. Audiol. 27, 195–203.

Khaitlina, S.Y., 2001. Functional specificity of actin isoforms. Int. Rev. Cytol. 202, 35–98.

Kikuchi, T., Takasaka, T., Tonosaki, A., Katori, Y., Shinkawa, H., 1991. Microtubules of guinea pig cochlea epithelial cells. Acta Otolaryngol. 111, 286–290.

Lim, D.J., 1986. Functional structure of the organ of Corti: a review. Hear Res. 22, 117–146.

Loomis, P.A., Zheng, L., Sekerkova, G., Changyaleket, B., Mugnaini, E., Bartles, J.R., 2003. Espin cross-links cause the elongation of microvillus-type parallel actin bundles in vivo. J. Cell Biol. 163, 1045–1055.

Matsubara, A., Laake, J.H., Davanger, S., Usami, S., Ottersen, O.P., 1996. Organization of AMPA receptor subunits at a glutamate synapse: a quantitative immunogold analysis of hair cell synapses in the rat organ of Corti. J. Neurosci. 16, 4457–4467.

Mahendrasingam, S., Furness, D.N., Hackney, C.M., 1998. Ultrastructural localisation of spectrin in sensory and supporting cells of guinea-pig organ of Corti. Hearing Res. 126, 151–160.

Micheva, K.D., Vallee, A., Beaulieu, C., Herman, I.M., Leclerc, N., 1998. β-Actin is confined to structures having high capacity of remodelling in developing and adult rat cerebellum. Eur. J. Neurosci. 10, 3785–3798.

Nakazawa, K., Schulte, B.A., Spicer, S.S., 1995. The rosette complex in gerbil Deiters' cells contains gamma-actin. Hearing Res. 89, 121–129.

Olson, E.S., Mountain, D.C., 1994. Mapping the cochlear partitions stiffness to its cellular architechture. J. Acoust. Soc. Am. 95, 395–400.

Oshima, T., Okabe, S., Hirokawa, N., 1992. Immunocytochemical localization of 205 kDa microtubule-associated protein (205 kDa MAP) in the guinea pig organ of Corti. Brain Res. 590, 53–65.

Otey, C.A., Kalnoski, M.H., Bulinski, J.C., 1987. Identification and quantification of actin isoforms in vertebrate cells and tissues. J. Cell Biochem. 34, 113–124.

Pataky, F., Pironkova, R., Hudspeth, A.J., 2004. Radixin is a constituent of stereocilia in hair cells. Proc. Natl. Acad. Sci. USA 101, 2601–2606.

Prassler, J., Stocker, S., Marriott, G., Heidecker, M., Kellermann, J., Gerisch, G., 1997. Interaction of a *Dictyostelium* member of the plastin/fimbrin family with actin filaments and actin–myosin complexes. Mol. Biol. Cell. 8, 83–95.

Robles, L., Ruggero, M.A., 2001. Mechanics of the mammalian cochlea. Physiol. Rev. 81, 1305–1352.

Rzadzinska, A.K., Schneider, M.E., Davies, C., Riordan, G.P., Kachar, B., 2004. An actin molecular treadmill and myosins maintain stereocilia functional architecture and self-renewal. J. Cell Biol. 164, 887–897.

Sato, N., Funayama, N., Nagafuchi, A., Yonemura, S., Tsukita, S., Tsukita, S., 1992. A gene family consisting of ezrin, radixin and moesin. Its specific localization at actin filament/plasma membrane association sites. J. Cell Sci. 103, 131–143.

Schneider, M.E., Belyantseva, I.A., Azevedo, R.B., Kachar, B., 2002. Rapid renewal of auditory hair bundles. Nature 418, 837–838.

Sheterline, P., Clayton, J., Sparrow, J.C., 1998. Actin Protein Profile. Academic Press, New York.

Skalli, O., Vandekerckhove, J., Gabbiani, G., 1987. Actin-isoform pattern as a marker of normal or pathological smooth-muscle and fibroblastic tissues. Differentiation 33, 232–238.

Slepecky, N.B., Chamberlain, S.C., 1982. Distribution and polarity of actin in the sensory hair cells of the chinchilla cochlea. Cell Tissue Res. 224, 15–24.

Slepecky, N.B., Chamberlain, S.C., 1983. Distribution and polarity of actin in inner ear supporting cells. Hearing Res. 10, 359–370.

Slepecky, N.B., Chamberlain, S.C., 1985. Immunoelectron microscopic and immunofluorescent localization of cytoskeletal and muscle-like contractile proteins in inner ear sensory hair cells. Hearing Res. 20, 245–260.

Slepecky, N.B., Chamberlain, S.C., 1986. Correlative immunoelectron-microscopic and immunofluorescent localization of actin in sensory and supporting cells of the inner ear by use of a low-temperature embedding resin. Cell Tissue Res. 245, 229–235.

Slepecky, N.B., Savage, J.E., 1994. Expression of actin isoforms in the guinea pig organ of Corti: Muscle isoforms are not detected. Hearing Res. 73, 16–26.

Slepecky, N.B., Ulfendahl, M., 1992. Actin-binding and microtubule-associated proteins in the organ of Corti. Hearing Res. 57, 201–215.

Tilney, L.G., DeRosier, D.J., Mulroy, M.J., 1980. The organization of actin filaments in the stereocilia of cochlear hair cells. J. Cell Biol. 86, 244–259.

Tolomeo, J.A., Holley, M.C., 1997a. Mechanics of microtubule bundles in pillar cells from the inner ear. Biophys. J. 73, 2241–2247.

Tolomeo, J.A., Holley, M.C., 1997b. The function of the cytoskeleton in determining the properties of epithelial cells within the organ of Corti. In: Lewis, E.R., Long, G.R., Lyon, R.F., Narins, P.M., Steele, C.R., Hecht-Poinar, E. (Eds.), Diversity in Auditory Mechanics. World Scientific, Singapore, pp. 556–562.

Vandekerckhove, J., Weber, K., 1978. At least six different actins are expressed in a higher mammal: an analysis based on the amino acid sequence of the amino-terminal tryptic peptide. J. Mol. Biol. 126, 783–802.

Vandekerckhove, J., Weber, K., 1981. Actin typing on total cellular extracts: a highly sensitive protein-chemical procedure able to distinguish different actins. Eur. J. Biochem. 113, 595–603.

Wijk, E., van Krieger, E., Kemperman, M.H., De Leenheer, E.M.R., Huygen, P.L.M., Cremers, C.W.R.J., Cremers, F.P.M., Kremer, H., 2003. A mutation in the gamma actin 1 (ACTG1) gene causes autosomal dominant hearing loss (DFNA20/26). J. Med. Gen. 40, 879–884.

Yao, X., Chaponnier, C., Gabbiani, G., Forte, J.G., 1995. Polarized distribution of actin isoforms in gastric parietal cells. Mol. Biol. Cell 6, 541–557.

Zheng, J., Shen, W., He, D.Z., Long, K.B., Madison, L.D., Dallos, P., 2000. Prestin is the motor protein of cochlear outer hair cells. Nature 405, 149–155.

Zhu, M., Yang, T., Wei, S., DeWan, A.T., Morell, R.J., Elfenbein, J.L., Fisher, R.A., Leal, S.M., Smith, R.J., Friderici, K.H., 2003. Mutations in the gamma-actin gene (ACTG1) are associated with dominant progressive deafness (DFNA20/26). Am. J. Hum. Genet. 73, 1082–1091.

Zine, E.A., Romand, R., 1993. Expression of alpha-actinin in the stereocilia of hair cells of the inner ear: immunohistochemical localization. NeuroReport 4, 1350–1352.